

Bionic Geomagnetic Navigation for Autonomous Underwater Vehicle with Temporal Attention-based Data-Driven Dead Reckoning

Songnan Yang, Xiaohui Zhang, Ding Liu, *Member, IEEE*, Wenqi Bai and Fan Liu

Abstract—Numerous studies have demonstrated that numerous animal species are capable of goal-directed navigation using environmental information for dead reckoning. The stable magnetic field of the earth provides important information for the migration of animals over long distances. Inspired by the goal-directed navigation of animals, a novel Geomagnetic Navigation with Temporal Attention-based Data-Driven Dead Reckoning (Attention-DR) method for Autonomous Underwater Vehicles (AUV) is presented in this article, which only utilizes the inclination angle (I) and the declination angle (D) of the Geomagnetic Field (GF) for underwater navigation without any prior knowledge of the geographical location or geographic map. This article proposes a Temporal Attention-based Long Short-Term Memory (TA-LSTM) neural network by combining history, GF information, and location in time series to achieve the optimization heading angle of underwater dead reckoning. Due to its ability to adjust the utilization weights of local and global temporal information in the path, TA-LSTM possesses the capability to continually update neural network model parameters through a data-driven process during the navigation process. This enables the Attention-DR to achieve efficient navigation in regions without prior magnetic maps and overcome navigation failures caused by magnetic field anomalies. The simulation outcomes confirm the efficiency, precision, and practicability of the proposed algorithm.

Index Terms—Geomagnetic navigation, autonomous underwater vehicle, data-driven control, dead reckoning, long short-term memory

This work was supported in part by the National Major Scientific Instrument Development Project of China under Grant 62127809; in part by the National Natural Science Foundation of China under Grant 62073258; and in part by the Basic Research in Natural Science and Enterprise Joint Foundation of Shaanxi Province under Grant 2021JLM-58. (*Corresponding author: Xiaohui Zhang.*)

S. Yang is with the School of Automation and Information Engineering, Xi'an University of Technology, Shaanxi 710048, China, and also with the Institute of Advanced Navigation and Electromagnetics, Xi'an University of Technology, Shaanxi 710048, China (e-mail: yang.son.nan@gmail.com).

X. Zhang and W. Bai are with the School of Automation and Information Engineering, Xi'an University of Technology, Shaanxi 710048, China, and also with the State Key Laboratory of Eco-Hydraulics in the Northwest Arid Region of China, Xi'an University of Technology, Shaanxi 710048, China (e-mail: xhzhang@xaut.edu.cn).

D. Liu and F. Liu are with the School of Automation and Information Engineering, Xi'an University of Technology, Shaanxi 710048, China, and also with the Shaanxi Key Laboratory of Complex System Control with the Intelligent Information Processing, Xi'an University of Technology, Shaanxi 710048, China (e-mail: liud@xaut.edu.cn).

Color versions of one or more of the figures in this article are available online at <http://ieeexplore.ieee.org>

I. INTRODUCTION

UNDERWATER navigation method provided accurate position, speed, and attitude information for Autonomous Underwater Vehicles (AUVs). Due to the rapid attenuation of radio frequencies in the underwater environment, the Global Navigation Satellite System (GNSS) is no longer suitable for AUVs. Numerous alternative methods, such as the Inertial Navigation System (INS), acoustic navigation, terrain-aided navigation, gravity-aided navigation, and geomagnetic navigation, have been utilized for AUV navigation. Despite the fact that INS is a passive method that does not rely on external information, its positioning error accumulates with time due to the error drift of inertial devices, preventing its use for long-distance underwater navigation [1]. Underwater acoustic navigation can provide high precision location information, but it requires the placement of signal beacons in advance, which is difficult to achieve in an unknown environment [2]. Underwater geophysical navigation methods mainly include terrain matching [3], gravity matching [4], and geomagnetic matching, with the characteristics of strong autonomy, good concealment, and area independence. The terrain contour matching (TERCOM) algorithm [5] for terrain matching navigation has been implemented in Tomahawk missiles [6] and gravity aided inertial navigation for underwater vehicles. TERCOM systems receive constant corrections throughout the movement processes and, as a result, do not have any drift. Magnetic contour matching (MAGCOM), which was the first proposed and widely used in magnetic navigation engineering practice [7], can only be used to calibrate the translation error because the initial heading error would produce a large position error. Therefore, the MAGCOM method is often used in conjunction with the inertial navigation system (INS) [8]. Another mainstream method of geomagnetic matching navigation based on the iterative closest contour point (ICCP) algorithm is also an important area of research in underwater navigation technology [9]. It is accomplished by following an optimal trajectory to match the real-time measured magnetic sequence desired in the geomagnetic map and correcting the translation and rotation errors, and it is first proposed for gravity matching [10][11]. Matching navigation generally refers to the similarity between the navigation trajectory sequence and the corresponding reference map, and the accuracy of navigation is largely depending on the setting of the matching step configuration. When a priori reference map cannot accurately reflect the geomagnetic characteristic environment of

the current navigation area, or when the AUV enters an unknown environment of the current navigation area without a high-precision geomagnetic map, the MAGCOM and ICCP methods will be severely constrained. Thus, traditional geomagnetic matching algorithms are limited by pre-stored map data, meaning that the entire route must be pre-planned, including its starting point, and that the accuracy and completeness of the maps are difficult to ensure for various reasons. Clearly, it is distinct from how marine animals navigate. It appears that marine animals lack a large-scale spatial distribution of the geographic information and only require the perceived real-time information while travelling.

Numerous marine organisms are known to migrate thousands of kilometers and return to their original environments. The distribution of water temperature, currents and pressure provides little information for marine animals to navigate [12][13]. Increasing evidence reveals that these animals use the Geomagnetic Field (GF) as a "map" to find their position and orient themselves [14]. "Magnetic displacement" experiments, in which animals are subjected to the magnetic intensity, inclination, or declination corresponding to the destination, while all other potential orientation cues—olfactory, inertial, visual, auditory, and so forth—are meticulously controlled and held constant [15]. These magnetic displacement experiments have yielded successful outcomes, illustrating that a diverse array of taxa, including crustaceans [16], fish [17], amphibians [18], reptiles [19], and birds [20], derive vital navigational information from the geomagnetic. Qi *et al.* [21] proposed an autonomous local navigation and positioning system without using magnetic field strength information. They simulated the magnetic dipole of the earth by using tilted magnets to generate a gradient magnetic field for navigation and positioning, employing a prediction algorithm based on the Extended Kalman Filter (EKF). However, significant changes in the local geomagnetic field, caused by external factors, may affect the accuracy of heading angle determination based on the gradient. Taylor *et al.* [22] proposed an agent-based computer simulation that uses the inclination of GF lines as a component of a magnetic compass sense for long-distance navigation. The results show that the sequential inclination and sequential inclination complement strategies are both capable of autonomous transequatorial migrations in both present-day and reversed magnetic fields. However, when the magnetic noise is introduced in both the polar and meridional directions, the strategy is affected to a degree that makes navigation impossible. So, combining the research of Qi, Taylor and other important relevant research [23][24], the question that has been difficult to resolve is how a consistent and reliable heading angle based on the GF gradient can resist the effects of the unknown magnetic field anomaly.

Various bionic geomagnetic navigation strategies have been proposed in research over the years to address this problem. Zhang *et al.* [25] proposed a geomagnetic gradient-assisted evolutionary algorithm for long-range underwater navigation. The geomagnetic gradient improves the evaluation function by limiting the evolutionary sample space to optimize navigation in the geomagnetic anomaly area. Simulations demonstrate that search efficiency and navigation path straightness are

considerably improved. Sample space constraint reduces navigation path search unpredictability. However, several computations during this process were ineffective searches, highlighting the need for a more thorough method beyond the monotonic decline of the objective function. Zhang *et al.* [26] proposed a long-distance underwater geomagnetic navigation method using the model predictive control (MPC) algorithm without any prior knowledge of the geographical location or geomagnetic map. This method not only showcases the potential of leveraging declination and inclination components for long-distance underwater geomagnetic navigation but also highlights the robustness of the MPC algorithm in mitigating the impact of various geomagnetic field anomaly. It is worth mentioning that the reliance on a single calculation of the gradient at the beginning of the navigation process, coupled with the subsequent updates based on acquired declination and inclination measurements, contributes to the adaptability and efficiency of the proposed approach. However, the impact of fixed Q and R parameters on the heading angle remains a critical consideration in achieving precise and accurate navigation in the presence of magnetic field anomalies. Wang *et al.* [27] proposed a tightly coupled integrated navigation model with EKF to fuse the information of the polarization compass and magnetometer for a bioinspired integrated navigation system. This method addressed the heading error of the system and enhanced local geomagnetic field reconstruction in magnetic anomalies. However, the complexity and scale of the polarization navigation system may make implementation difficult, warranting further investigation.

In this study, we propose that the historical geomagnetic data obtained during the navigation process can be treated as a time series dataset. From this dataset, it is possible to extract the changing trends of the magnetic field gradient in the current region. In this context, neural network-based techniques have emerged as useful, cutting-edge methods to address the heading angle error cost of magnetic anomalies. By combining the history and current GF information, we can estimate the intensity of the magnetic field anomalies. To accomplish this, we introduce a data-driven heading angle estimation method based on a Temporal Attention-based Long Short-Term Memory (TA-LSTM) neural network. By incorporating a well-designed heading constraint strategy, we aim to address the limitations of existing methods such as the EKF, MPC and evolutionary computation, which are known to be significantly affected by magnetic field anomalies. Our proposed Attention-DR method seeks to overcome the gradient disappearance problem caused by magnetic field anomalies and enhance the reliability and efficiency of the navigation system by leveraging the predictive capabilities of the TA-LSTM neural network in estimating the heading angle.

The rest of this article is organized as follows. In Section II the mathematical description of the GF information formulates the problem of bionic geomagnetic navigation. Section III presents a data-driven model predictive control algorithm to provide the correct heading angle for AUVs navigating underwater magnetic field anomalies. And the navigation performance of the proposed method is analyzed and compared following the simulations in Section IV. Conclusions are offered in Section V.

II. FUNDAMENTALS

A. Description of the Geomagnetic Field Information

The Geomagnetic Field (GF) is a basic physical field of the earth, and it is mainly composed of three parts. The main magnetic field B_m , produced by largescale electric currents in the liquid outer core of the earth, consisting of conductive molten irons [28]. The B_m changes very slowly and the time cycle is measured on the scale of a thousand years. The magnetic field anomaly B_e , mainly generated from ferrimagnetic minerals, which decaying with height, and hardly changes with time. The disturbed magnetic field B_d , originating in the ionosphere and magnetosphere, which varies dramatically over time and is always associated with solar activity [29]. It follows that the value of the magnetic field B at any place on the earth is:

$$B(t) = B_m(t) + B_e(t) + B_d(t) \quad (1)$$

There are seven elements that make up the main GF vector B_m . As is shown in Fig. 1, these are the northerly intensity B_x , the easterly intensity B_y and the vertical intensity B_z derived from B_x, B_y, B_z : the horizontal intensity H , the total intensity F , the inclination angle I and the declination angle D . The axis of the magnetic pole currently tilts at an angle of 11° with respect to the axis of rotation, as if a magnetic bar were situated at that angle in the center of the earth. Consequently, the horizontal direction of the GF does not coincide with the direction of geographic north in most cases.

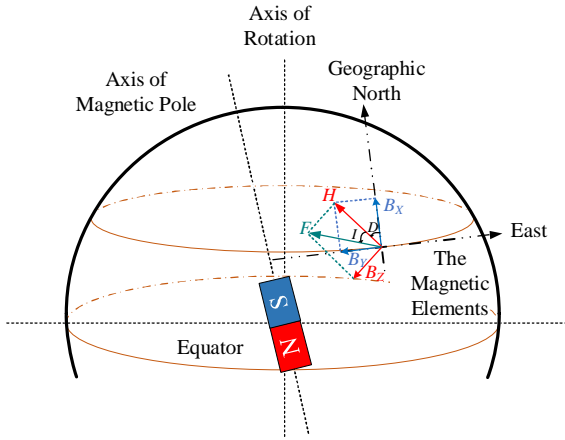


Fig. 1 Seven elements of the main geomagnetic field vector B_m associated with an arbitrary point in space.

Various models can be used to characterize the main GF of the earth, such as the world magnetic model (WMM) [30], the international geomagnetic reference field model (IGRF) [31], and the enhanced magnetic model (EMM) [32]. The scientific community employs these models to investigate space weather, electromagnetic induction, and local magnetic anomalies. It is also extensively employed in satellite attitude determination and control systems, as well as other applications requiring orientation information. In this article, instead of measuring GF with a triaxial magnetometer, we choose the WMM2020 model to get the GF information. In practical applications, values obtained from both sensors and theoretical models can be used with proposed method. The number of inclination angle I and the declination angle D are

calculated by feeding the WGS84 coordinates into the WMM2020 model and transformed to the Universal Transverse Mercator (UTM) coordinate system using Gaussian projection for AUV navigation. The transformation method in this article refers to the research by Wu *et al.* [33].

Theoretically, the geomagnetic vector at any given location corresponds to its geographical position in the earth, one by one [34]. On the ground, the GF intensity ranges from approximately 25000 to 65000 nT [35]. Given that three of the seven elements can be calculated by using (2). In this article, the TA-LSTM method uses the geomagnetic information provided by D and I . By convention, the D is positive when the magnetic north is to the east of the geographic north, and the negative when it is to the west. The positive values of I indicate that the GF at the site of measurement is pointing downward into the earth, while negative values indicate that it is pointing upward [30]. Therefore, when using D and I to calculate the geomagnetic gradient, it is necessary to change the positive or negative values according to the direction of travel to find the correct heading angle.

$$\begin{aligned} B_x &= F \cos I \cos D \\ B_y &= F \cos I \sin D \\ B_z &= F \sin I \\ F &= \sqrt{B_x^2 + B_y^2 + B_z^2} \\ H &= F \cos I \\ I &= \arccos(H / F) \\ D &= \arccos(B_x / H) \end{aligned} \quad (2)$$

B. Problem Description

The GF is comprised of multiple elements, and the GF information corresponds to the geographical location, providing solid physical foundation for bionic underwater navigation. In this article, the geomagnetic elements at a position in the trajectory are described as:

$$S = \{S_o, S_1, \dots, S_{k-1}, S_k, S_{k+1}, \dots, S_d\} \quad (3)$$

where the D and I at the k th sampling location are denoted by $S_k = [D_k, I_k]^T$. Simultaneous, the $S_o = [D_o, I_o]^T$ and the $S_d = [D_d, I_d]^T$ represent the D and I at the starting location and the destination, respectively. The underwater navigation process from the starting location to the destination. During the navigation, the S_k can be obtained by magnetometer while arriving a new sampling location L_k . The trajectory of navigation is described as:

$$L = \{L_o, L_1, \dots, L_{k-1}, L_k, L_{k+1}, \dots, L_d\} \quad (4)$$

where $L_o = [lx_o, ly_o]^T$ and $L_d = [lx_d, ly_d]^T$ represents the starting location and the destination. The lx_k and ly_k are represents the coordinates in the xoy coordinate frame, and the values can be obtained by assuming a motion model:

$$\begin{aligned} lx_{k+1} &= lx_k + \cos y_N^k \mathcal{V}_k \\ ly_{k+1} &= ly_k + \sin y_N^k \mathcal{V}_k \end{aligned} \quad (5)$$

where y_N^k is the heading angle at k th sampling time of 1 second movement with velocity \mathcal{V}_k . The heading angle, which determines the movement direction of the AUV, and the velocity determines the distance traveled in this direction, are the key factor for navigating and have some connection in

time sequence. To correlate GF information with heading angle, the geomagnetic gradient information is used to calculate two adjacent moments D and I by the following equation:

$$\begin{cases} D_{k+1} = D_k + g_{D_{xk}} \cos q_k + g_{D_{yk}} \sin q_k \\ I_{k+1} = I_k + g_{I_{xk}} \cos q_k + g_{I_{yk}} \sin q_k \end{cases} \quad (6)$$

where $g_{D_{xk}}, g_{D_{yk}}, g_{I_{xk}}, g_{I_{yk}}$ are the gradients of D and I . The k th gradients are obtained through a simple decomposition of the changes of D and I in the East and North directions [25][26]. The geomagnetic gradient of can be calculated by the $k+1$ th, k th and $k-1$ th geomagnetic elements measured by magnetometer or bring the WGS84 geographic coordinates into the WMM model for solution:

$$\begin{cases} g_{D_{xk+1}} = \frac{D_k - D_{k-1}}{l_{x_k} - l_{x_{k-1}}} \\ g_{D_{yk+1}} = \frac{D_{k+1} - D_k}{l_{y_{k+1}} - l_{y_k}} \\ g_{I_{xk+1}} = \frac{I_k - I_{k-1}}{l_{x_k} - l_{x_{k-1}}} \\ g_{I_{yk+1}} = \frac{I_{k+1} - I_k}{l_{y_{k+1}} - l_{y_k}} \end{cases} \quad (7)$$

The calculate heading angles can be obtained as follows:

$$y_N^k = \arctan\left(\frac{(I_k - I_d)g_{D_{xk}} - (D_k - D_d)g_{I_{xk}}}{(D_k - D_d)g_{I_{yk}} - (I_k - I_d)g_{D_{yk}}}\right) \quad (8)$$

where the gradients $g_{D_{xk}}, g_{D_{yk}}, g_{I_{xk}}, g_{I_{yk}}$ can be calculated by (7). Therefore, by constructing a reasonable objective function and describing its convergence process can determine whether the AUV reaches its destination:

$$f_i(S_k) = \frac{(S_{i,k} - S_{i,d})^2}{(S_{i,0} - S_{i,d})^2} \quad (9)$$

where, $f_i(S_k)$ is the i th geomagnetic elements at k th time and destination. To exclude differences of magnitude and units, the objective function is normalized to:

$$F(S_k) = \frac{1}{n} \sum_{i=1}^n f_i(S_k) \quad (10)$$

When the AUV arrives at the destination, theoretically, the objective function is zero. However, to prevent the search for unique solutions from taking too much time, the navigation process is terminated when the error converges to e considered the AUV to have reached the destination. This is expressed as:

$$F(S_k) \leq e \quad (11)$$

Marine organisms can use GF information to discover magnetic field abnormalities in navigation routes and change their heading angle. The theoretical model shows that heading angle and velocity are the most important geomagnetic navigation parameters. The GF information and position sequence strongly correlate with the history data of the navigation phase. Therefore, based on this idea, this article proposes an Attention-DR navigation method based on Temporal Attention-based LSTM (TA-LSTM) neural network that utilizes a period of sample data during the navigation process to predict the GF information and compare it with the

actual GF information, as shown in Fig. 2. By determining whether a given navigational region is within an abnormal zone and using a data-driven method to adjust the actual heading angle by predicting the heading angle, the proposed approach is able to achieve stable, fast, and accurate convergence of multiple geomagnetic parameters during the navigation process.

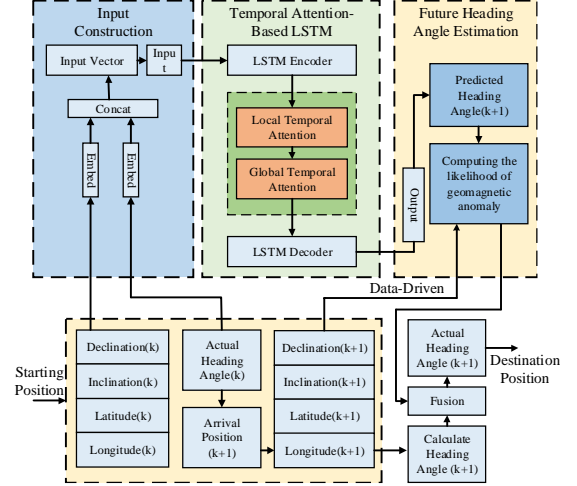


Fig. 2 Schematic diagram of geomagnetic navigation with temporal attention-based data-driven dead reckoning.

III. PROPOSED ATTENTION-DR NAVIGATION METHOD

To achieve the Temporal Attention-based Data-Driven Dead Reckoning (Attention-DR) navigation method, the Declination Component (D) and Inclination Component (I) of the destination have been known before the navigation. The D and I at any location on the earth can be known by the magnetometer in real time. The hypotheses here are the same as [26][27]. Unlike [26][27], we not only use the D and I measured in real time to compare with the D and I at the destination to determine whether the destination is reached or not, but also use the sequence of D and I to train the TA-LSTM network model for the prediction of GF information and heading angle. The heading angle and attitude of the AUV relative motion can be obtained by the precise inertial navigation system (INS), which has been studied and widely used in aviation, aerospace and underwater navigation for several years [36][37][38].

First of all, the process of Attention-DR is described. The gradient of D and I at the origin is required at the beginning of the navigation. As is shown in Fig. 3, the AUV moves towards x from starting location L_0 for the velocity V_1 in the xoy coordinate to L_1 . Then move towards y from L_1 for the velocity V_2 . This process is designed to be utilized (7) to compute the initial gradient. The historic sequence of D and I at each location is saved and used to calculate the heading angle and train the TA-LSTM network. Until the training process is complete, the heading angle can be generated using inertial navigation, or the WMM geomagnetic model without anomaly. The geomagnetic navigation iterates until the objective function converges (10) less than the pre-set value. The Attention-DR method proposed in this article uses historical geomagnetic data and the heading angle training

TA-LSTM network and fuses the predicted heading angle with the calculate heading angle, which can effectively resist the great influence of magnetic field anomalies on navigation. In the following, the method will be introduced in detail.

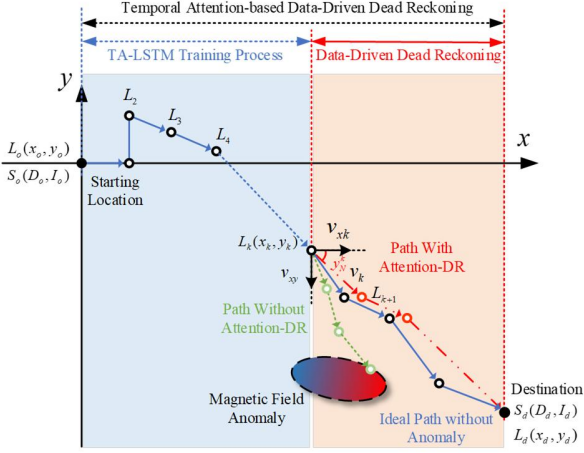


Fig. 3 The geomagnetic navigation process with temporal attention-based data-driven dead reckoning.

A. Description of the Long Short-Term Memory.

Long Short-Term Memory (LSTM) neural network, as described by [39], is a type of Recurrent Neural Network (RNN) that addresses the problem of disappearing gradient in RNNs by introducing gating mechanism. With the help of memory unit and gate mechanism. LSTM is capable of extracting the inherent patterns within a series that exhibit longer intervals and delays, thanks to its utilization of cell memory and hidden state mechanisms [40]. The LSTM consists of hidden state h_k and cell memory c_k , that respectively stores the summary of the past input sequence and controls the information flow between the input and output through gating mechanism. The LSTM computes as follows:

$$f_k = s(W_f \bowtie h_{k-1}, x_k] + b_f) \quad (12)$$

$$i_k = s(W_i \bowtie h_{k-1}, x_k] + b_i) \quad (13)$$

$$o_k = s(W_o \bowtie h_{k-1}, x_k] + b_o) \quad (14)$$

$$g_k = \tanh(W_g \bowtie h_{k-1}, x_k] + b_g) \quad (15)$$

$$c_k = f_k \mathbf{e} c_{k-1} + i_k \mathbf{e} g_k \quad (16)$$

$$h_k = o_k \mathbf{e} \tanh(c_k) \quad (17)$$

where, f_k, i_k and o_k are gating vectors, that respectively control how much information for the cell memory to forget, update and output. s is a logistic sigmoid function, \mathbf{e} is element wise product and x_k is the input vector. Where W_f, W_i, W_o and W_g are linear transformation matrices whose parameters need to be learned, while b_f, b_i, b_o and b_g are corresponding bias vectors. We simplify the basic LSTM representations as follows:

$$(h_k, c_k) = LSTM(x_k, h_{k-1}, c_{k-1}) \quad (18)$$

B. Description of the GF information encoder with local temporal attention and decoder with global temporal attention.

A notable characteristic of marine animal perception is its tendency to selectively process external stimuli rather than instantaneously attending to all inputs. In contrast, animals will initially prioritize the salient components in order to extract the

necessary information [41]. The attention mechanism possesses the ability to dynamically choose the most pertinent input characteristics and provide greater importance to the associated original feature sequence. Inspired by the marine animal navigation in long-range, we proposed to use the temporal attention mechanism extracts reliable underwater GF information for navigation by adaptively paying more local attention to relevant heading angle of encoder during future sequence generation, and adaptively greater global attention to relevant hidden state. We assume that the entire input sequence of length nT is divided into n interval ranges by period T to achieve TA-LSTM. The GF information is separately fed into the LSTM networks to extract features. It has been observed that there is a strong correlation between the heading angle and the time series data of GF information and AUV geographic location. The temporal attention mechanism assigns larger weights to heading angle sequences that have stronger correlations with the projected destination position. Consequently, the temporal attention mechanism can be utilized to analyze potential patterns in the geomagnetic information-location relationship and heading angle sequences in order to solve the problem of undetermined heading caused by the disappearance of geomagnetic gradients and geomagnetic anomalies during AUV navigation.

The GF information $S_k = [D_k, I_k]^T$ and the AUV sampling location $L_k = [x_k, y_k]$ are represented as a series of time-stamped vector, and the dead reckoning problem can be framed as that of heading angle prediction, so it can be treated as a sequence to sequence (Seq2Seq) problem. Assuming that the input data sequence is $X = [X_1, X_2, \dots, X_n, \dots, X_N]$, the sequences of n -th local GF information and location are embedded as $X_n = [x_1^n, x_2^n, \dots, x_T^n]$ to the encoder process, where $x_k^n = [L_k^n, S_k^n]$ represents the k -th visited location and GF information, and the actual heading angle will be used as the feature sequence for training $Y_n = [y_1^n, y_2^n, \dots, y_T^n]$, where $y_k^n = q_k^n$ is the k -th actual heading angle of n -th local that the AUV will navigation in order. The sequence prediction model aims to learn a nonlinear relationship between GF information, location and heading angle. The problem of (10) is formulated as $Y = F(X)$, where $F(\cdot)$ is the nonlinear function the data-driven process aims to learn.

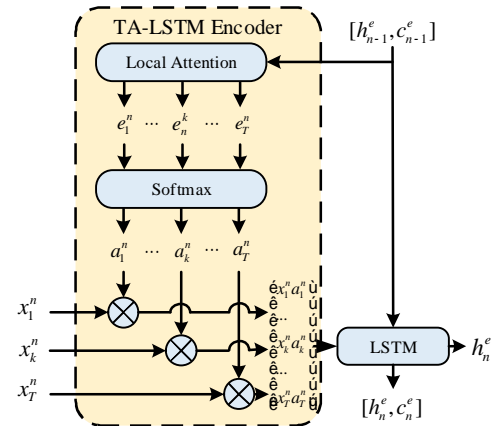


Fig. 4 The structure of encoder with local temporal attention.

The TA-LSTM encoder-decoder structure is based on two LSTM process, the encoder structure as is shown in Fig. 4 and the decoder structure as is shown in Fig. 5. The encoder process recursively inputs the sequence x_n^n of length T and update the encoder state vector c_n^e and h_n^e at each n -th local through (18), and summarizes the whole input sequence into the vectors c_N^e and h_N^e . The local temporal attention weights of local feature on the actual heading angle e_k^n and the important degree of GF information a_k^n are as follows:

$$e_k^n = V_e^T \times \tanh(W_e \times [h_{n-1}^e, c_{n-1}^e] + U_e \times Y_n + b_e) \quad (19)$$

$$a_k^n = f_{\text{softmax}}(e_k^n) \quad (20)$$

where $f_{\text{softmax}}(*)$ is a non-linear activation function, V_e^T , W_e , U_e and b_e are the parameters of local attention need to be learned, a_k^n is the local attention weight. The local attention mechanism reconstructs the information of the actual heading angle to participate in the temporal training of LSTM. Then, the hidden state from the TA-LSTM encoder h_n^e are as follows:

$$(h_n^e, c_n^e) = \text{LSTM}(\bar{X}_n, h_{n-1}^e, c_{n-1}^e) \quad (21)$$

where $\bar{X}_n = (x_1^n \times a_1^n, x_2^n \times a_2^n, \dots, x_T^n \times a_T^n)$ is the input GF information with local attention weight. The LSTM decoder process uses the cell memory c_n^e and hidden state h_n^e from the encoder. The initial state for the decoder process of the cell memory are $c_0^d = c_N^e$ and hidden state $h_0^d = h_N^e$. The global temporal attention weight of hidden layer state from encoder every n -th location of GF information important degree are as follows:

$$l_t = V_d^T \times \tanh(W_d \times [h_{n-1}^d, c_{n-1}^d] + U_d \times h_t^e + b_d) \quad (22)$$

$$b_t = f_{\text{softmax}}(l_t) \quad (23)$$

$$c_n^d = \sum_{t=1}^n b_t h_t^e \quad (24)$$

where V_d^T , W_d , U_d and b_d are the parameters of global attention need to be learned, b_t is the global attention weight.

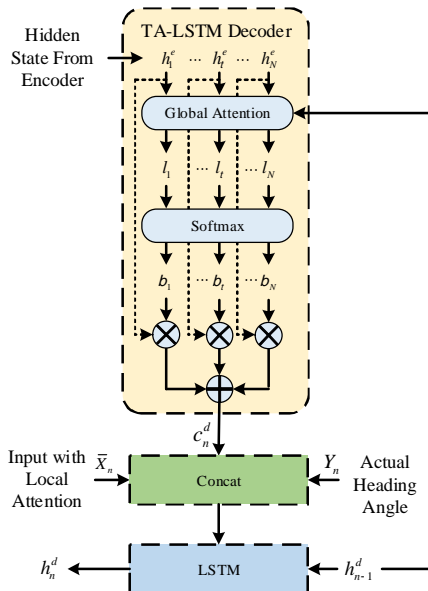


Fig. 5 The structure of decoder with Global temporal attention.

To integrate all the GF information sequence data, we use Fully Connected (FC) feedforward neural network to combining the local temporal attention weight a_k^n and global temporal attention weight c_n^d , the input of decoder Y_n with global attention

are obtained as follows:

$$Y_n' = W_n \times [\bar{X}_n, c_n^d, Y_n] + b' \quad (25)$$

where W_n and b' are the weight parameters of the first FC for input integration. The hidden state of the decoder are as follows:

$$h_n^d = \text{LSTM}(Y_n', h_{n-1}^d) \quad (26)$$

After N iterations, the final cell memory c_N^d and hidden state h_N^d are used to calculate the predicted value. Therefore, the $N+1$ -th predicted heading angle can be calculated as follows:

$$\bar{Y}_{N+1} = V_y^T \times (W_y \times [h_N^d, c_N^d] + b_w) + b_y \quad (27)$$

where W_y and b_w are the weight parameters of the second FC layer for output integration; V_y^T and b_y are the weight parameters of the third single FC for dimension transformation. The model set involved in the TA-LSTM is defined as f . All the parameters learned are updated to get the optimal prediction heading angle, aiming at minimizing the loss function as follows:

$$\text{loss}(f) = \frac{1}{M} \sum_{m=1}^M (y_{N+1}^m - \bar{y}_{N+1}^m)^2 \quad (28)$$

where, M is the number of validation sets, y_{N+1}^m and \bar{y}_{N+1}^m are the actual and predicted heading angles of the m -th validation sample, respectively. It is essential to maintain a global perspective throughout the entire navigation process in order to avoid an overemphasis on local geomagnetic gradients and the possibility of magnetic field anomaly entanglement. Therefore, the proposed TA-LSTM with local and global temporal attention mechanisms facilitates more accurate predictions than the traditional LSTM.

C. Computing the likelihood of geomagnetic anomaly and updating the actual heading angle.

Since the accuracy of the TA-LSTM for predicting heading angle is highly dependent on the number of samples and limited by the sampling speed of the magnetometer sensors, there is less data available for network training in the early stages of navigation. To make the quickest determination of whether an AUV is in a magnetic field anomaly. We employ Maximum Likelihood Estimation (MLE) to determine whether the current position is within a geomagnetic anomaly region. Based on this strategy, we have designed an anomaly score to update the actual heading angle. The error vectors at the N -th location are as follows:

$$e^N = \frac{1}{k} \sum_{k=1}^k |\bar{y}_N^k - y_N^k| \quad (29)$$

where y_N^k and \bar{y}_N^k represent the calculate and predicted heading angles of the k -th time. By assuming $y_N^k : N(m, s^2)$, the N -th calculate heading angle sequences are used to estimate the parameters m and s^2 by using MLE. For any interval of the heading angle, the anomaly score computes as follows:

$$h^N = \exp\left(-\frac{(e^N - m)^T (m - e^N)}{s^2}\right) \quad (30)$$

When the AUV arrives in the unknown magnetic anomaly place, the anomaly score decrease, indicates a dramatic GF information change in the anomaly the area, the actual heading angle the AUV update as follows:

$$y_N^k = h^N \times y_N^k + (1 - h^N) \times \bar{y}_N^k \quad (31)$$

The complete Attention-DR algorithm is summarized in Algorithm 1.

Algorithm 1 Attention-DR for Geomagnetic Navigation

Input: $S_o = [D_o, I_o]^T$ (Starting state), $S_d = [D_d, I_d]^T$ (Destination state), $L_o = [x_o, y_o]$ (Starting Location), $L_d = [x_d, y_d]$ (Destination Location), e (Terminated error converges), V_o (Starting Velocity).

- 1: Initial input data sequence X_1 and heading angle feature sequence Y_1 by (2)-(8) and WMM2020.
- 2: **for** $n=1; n < N$
- 3: **while** $F(S_{k+1}) > e$ **do**
- 4: Calculate Heading Angle y_n^k
- 5: TA-LSTM Encoder:
 Learn the LSTM parameters by (12)-(17) and local attention weight by (19)-(20) with the loss function set by (28).
 Update the encoder cell and hidden state c_n^e and state h_n^e by (21).
- 6: TA-LSTM Decoder:
 Learn the LSTM parameters by (12)-(17) and local attention weight by (22)-(24) with the loss function set by (28).
 Calculate the decoder output by (25), then update the decoder cell and hidden state c_n^d and state h_n^d by (26).
 Update predicted heading angle \bar{y}_{n+1}^k by (27).
- 7: Calculate geomagnetic anomaly score and updating the actual heading angle y_n^k by (29)-(31).
- 9: Update Location L_{k+1} and S_{k+1} with y_n^k
- 10: Set $V_{k+1} = lr(V_o)$, lr denotes the decay with iteration.
- 11: **end while**
- 12: **end for**

IV. SIMULATION

In this section, the simulations are carried out to verify the performance of the proposed Attention-DR navigation method. All simulations are performed on a desktop computer (CPU: Intel Core i7-11700; 2.50Ghz; RAM: 16Gb; Graphics: GTX1060; 6Gb) using a software developed on MATLAB R2023a platform. In these simulations, we choose a rectangular area in the vast western Pacific, which is from 20° north latitude, 130° east longitude (20°N, 130°E) to 30° north latitude, 140° east longitude (30°N, 140°E). According to the WMM 2020, the geographical coordinates of the area can be uniquely determined by the GF information.

In the following three simulation test, the GF information are retrieved from the WMM2020 model. At the beginning of the navigation, the AUV need to move, the heading angles are set as 0° and 90°, respectively, and the geomagnetic gradient is calculated from (7). At the initial state of navigation, the heading angles calculated from (8) are considered as the feature sequence. The TA-LSTM network training process was conducted in a region without geomagnetic field anomaly and in a region where interference is generated using the multimodal function to facilitate the replication of the experimental results. From the research of Zhang [26], we know that using declination (D) and inclination (I) in geomagnetic information requires the AUV to be at a suit able moving speed at the beginning, if the speed is too slow the

actual geomagnetic gradient cannot be obtained, and too fast is wasting of time and cost.

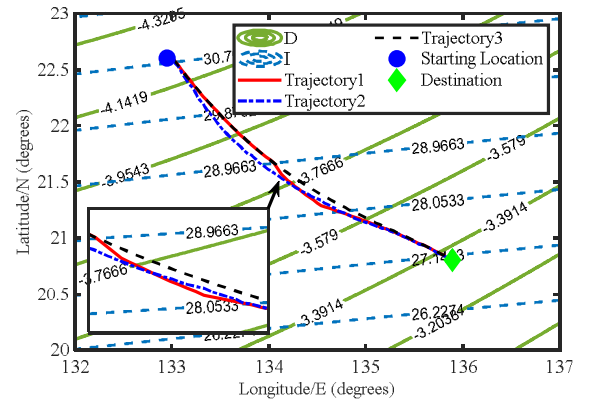
To facilitate the comparison of experiment performance, we chose initial speed V_0 is 40 knots (about 74.08 km/h). At the navigation process carries on, the AUV keeps approaching the destination. Letting the geomagnetic parameters converge faster and improve the accuracy of the process, this paper sets the speed decay of the initial speed the k -th speed is as follows:

$$V_k = \begin{cases} V_0 \cdot \text{drate}^{\frac{\text{int}(\frac{k-itr}{\text{destep}})}, & |lat_{itr} - lat_d| \leq 0.5^\circ \& |lon_{itr} - lon_d| \leq 0.5^\circ \\ V_0, & \text{else} \end{cases} \quad (32)$$

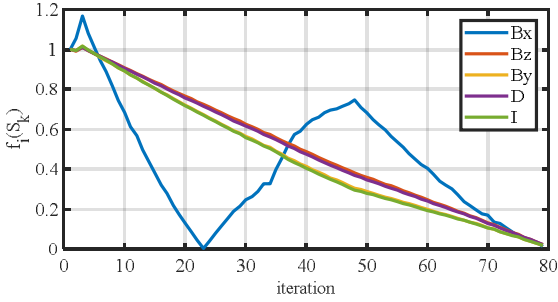
where, lat_{itr} and lon_{itr} indicates the itr -th forward reaching within 0.5° to the destination of lat_d and lon_d , the conversion relationship between latitude, longitude and xoy distance can be obtained by using the Great circle distance [42], int means rounded down to the nearest integer, destep indicates the initial speed decay interval with drate as the decay rate.

A. Simulation without geomagnetic field anomaly

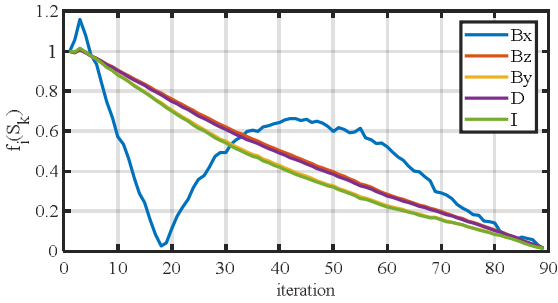
In this article, we choose (22.6°N, 132.95°E) as the starting location and (20.8°N, 135.89°E) as the destination for simulation without interference, the starting state is $S_o = [-4.2220, 30.8672]^T$ and the destination state is $S_d = [-3.6444, 28.8878]^T$ and the position in xoy is $L_o = [-7.2298 \times 10^5, -2.7052 \times 10^4]^T$. To prove the effectiveness of the proposed method, in addition, the simulations in this part are carried out in Attention-DR, original LSTM without attention, and the evolutionary method proposed by Zhang [25]. The rest of the parameters for Attention-DR and original LSTM are set as follows: $T=30$, $N=10$, $\text{epoch}=50$, $\text{numhidden}=100$, $\text{minibatch}=24$, $\text{Learning Rate}=0.005$, $\text{LearnDropFactor}=0.9$, $\text{TrainRatio}=0.7$ and $\text{ValidationRatio}=0.2$. The parameters of evolutionary method are consistent with Zhang [25]. The terminated condition for all methods when $e=0.02$ or maximum of 300 iterations.



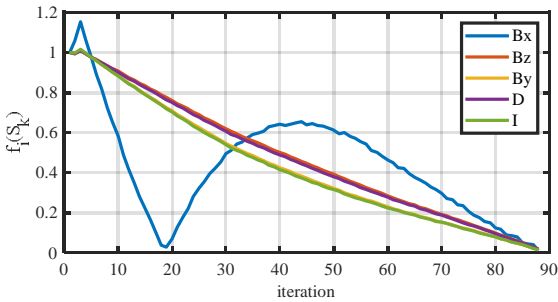
method [26] with the final arrival location of (20.839°N, 135.840°E) in 89 steps and total traveled 378.376km. The Trajectory 3 is the result of the original LSTM method with the final arrival location of (20.822°N, 135.816°E) in 88 steps and total traveled 376.243km. From the comparative analysis of the results, it becomes evident that the Attention-DR method requires fewer iterations compared to the other two approaches. Moreover, it exhibits a shorter total traveled distance and maintains closer proximity to the destination. Due to the introduction of temporal attention, more significant GF features will be focused on during the journey to shorten the traveled distance. To further illustrate the advantage, the geomagnetic elements convergence is analyzed as below.



(a) Convergence curve of geomagnetic elements in trajectory 1.



(b) Convergence curve of geomagnetic elements in trajectory 2.



(c) Convergence curve of geomagnetic elements in trajectory 3.

Fig. 7 Convergence curve of geomagnetic elements.

As shown in Fig. 7, the proposed Attention-DR method produces a significantly faster convergence performance than the evolutionary and original LSTM methods. In the initial stage of navigation, there is not enough priori information for Attention-DR and original LSTM training, thus the trajectories of these two methods overlap. When the training is complete, we can clearly find that the heading angle using the Attention-DR method has changed, moving towards to evolutionary method, but with a more stable heading. This is because, despite the fact that the evolutionary approach computation obtains the optimal heading

based on geomagnetic information, the search sensitivity of the process is relatively high, causing the heading angle to change too rapidly. In addition, the range of heading constraints and the randomness of optimum population selection are reduced due to the obstacles, reducing the navigational efficiency. Once a sufficient quantity of geomagnetic data is collected, the benefits of the Attention-DR method become apparent, and it is observed that the convergence of Trajectory 1 is continuous, smooth, and highly predictable. However, environments without anomaly are uncommon in the real world, so we continued the simulation with anomaly to evaluate the efficacy of Attention-DR.

B. Simulation with geomagnetic field anomaly.

The geomagnetic anomaly arises from the heterogeneity in the distribution of magnetic materials inside the Earth's crust, hence causing fluctuations in both the magnitude and intensity of the anomaly field. These anomalies can range from weak fields with strengths below 1 nT to strong fields several times stronger than the main magnetic field. From the model of (1), the presence of magnetic anomalies alters the spatial distribution characteristics of normal geomagnetic field parameters, generating strong interference to the heading angle of navigation. Encountering geomagnetic anomalies is an inevitable occurrence during navigation. Therefore, it is crucial to analyze the performance of the proposed and compared methods in the presence of geomagnetic anomalies through simulations. This has an immediate impact on the utility of the methodology.

The variation of geomagnetic anomaly field on earth is complex, changeable and unpredictable. In anomalous fields, the use of navigation methods relying on geomagnetic gradient information may encounter problems of gradient vanishing and falling into local optimization leading to navigation failure. As is shown in Fig. 8, three examples illustrate situations with different angles between contours, arrows show the gradient directions towards the destination for each of the contours of the GF Declination (D) and Inclination (I).

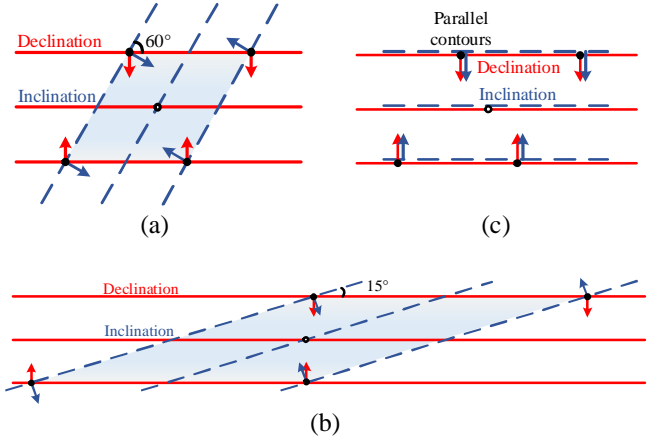


Fig. 8 The schematic diagram depicts the influence of angular disparity between contours on the process of geomagnetic navigation from a remote site to a desired destination.

From Fig. 8(a), it can be observed that when the angle between D and I is large, significant geomagnetic gradient information can be utilized to determine the heading angle. However, this may result in the AUV getting trapped in

regions with magnetic anomalies. On the other hand, when the angle between D and I decrease, as shown in Fig. 8(b), the geomagnetic gradient information becomes highly susceptible to disturbance caused by angle variations, and it may even lead to a 180° deviation in the heading. Additionally, when D and I are parallel, as is shown in Fig. 8(c), it becomes impossible to determine the heading angle using geomagnetic gradients. These situations are likely to occur in regions with magnetic anomalies. When calculating heading position by position, geomagnetic data will directly determine the heading, whereas when analyzing all historical data, the underlying pattern of geomagnetic variations will assist the AUV in escaping anomalous regions.

To simulate the aforementioned magnetic anomaly situations to the maximum extent and facilitate experimental reproducibility, we utilized a multimodal function to generate anomalies, as is shown in Fig. 9, the geomagnetic field anomaly was superimposed on top of the basic WMM2020 model. The mathematical representation of the anomaly can be expressed as follows:

$$B_e = 3 \times (1-x)^2 \times e^{(-x^2-(y+1)^2)} - 10 \times \frac{x}{5} - x^3 - y^5 \times e^{(-x^2-y^2)} - \frac{1}{3} \times e^{(-(x+1)^2-y^2)} \quad (33)$$

By adding 200 times B_e in the B_x direction, 400 times B_e in the B_y direction, and 600 times B_e in the B_z direction, as is shown in Fig. 9. Then utilizing (2) to calculate the other geomagnetic elements, a complete magnetic anomaly region was constructed. For the simulation tested the performance of the Attention-DR and comparative methods, during navigation process this area does not have a priori knowledge.

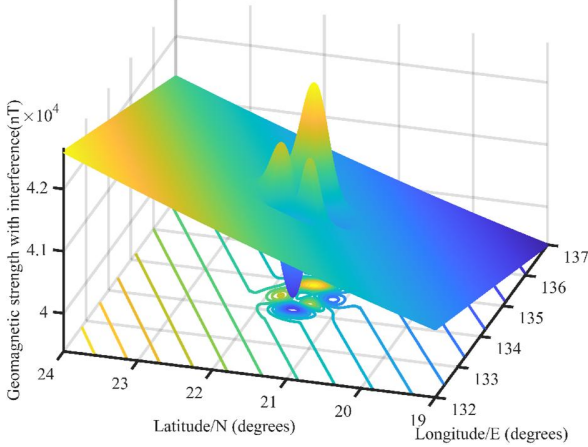


Fig. 9 Geomagnetic field anomaly in navigation area.

The simulation trajectories with anomaly are as shown in Fig. 10, and the convergence of geomagnetic elements are as shown in Fig. 11. From starting location (22.6°N , 132.95°E) to the destination (20.8°N , 135.89°E), the Trajectory 1 is the result of the Attention-DR proposed in this article with the final arrival location of (20.841°N , 135.813°E) in 87 steps and total traveled 383.833km. The Trajectory 2 is the result of the evolutionary method [26] with the final arrival location of (21.303°N , 133.880°E) in 299 steps and total traveled 801.153km. The Trajectory 3 is the result of the original LSTM method with the final arrival location of (20.822°N , 135.816°E) in 299 steps and total traveled 376.243km.

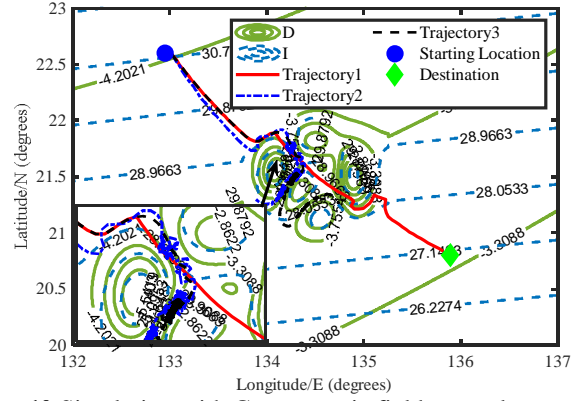
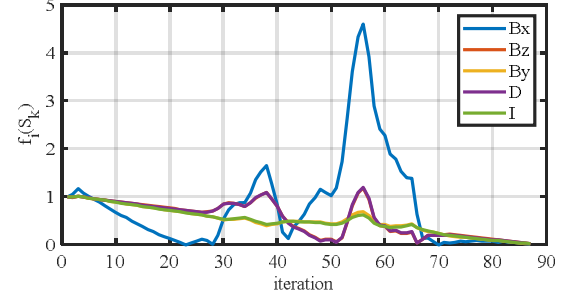
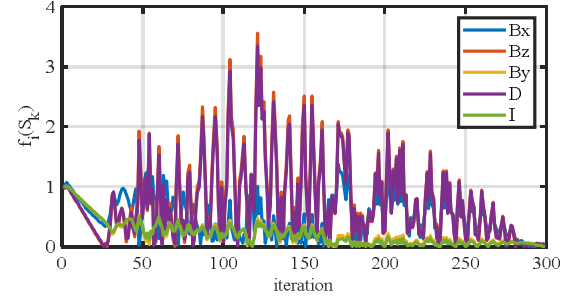


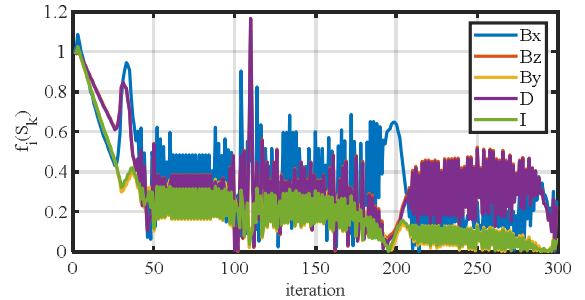
Fig. 10 Simulation with Geomagnetic field anomaly.



(a) Convergence curve of geomagnetic elements in trajectory 1.



(b) Convergence curve of geomagnetic elements in trajectory 2.



(c) Convergence curve of geomagnetic elements in trajectory 3.

Fig. 11 Convergence curve of geomagnetic elements.

It is evident that within a limited time frame, the Attention-DR method successfully overcomes the interference caused by the magnetic anomalies, avoiding getting trapped within the anomalous region during the navigation process. While the other two methods failed to reach their destination in the limited iteration. As can be seen from Fig. 10, Trajectory 1, Trajectory 2 and Trajectory 3 are consistent with the results in the initial stage without interference. When the AUV just enters the anomalous region, the heading calculated by the three methods are affected

by the anomalous region, but as the AUV goes further, the Attention-DR method is able to utilize the anomaly score to amendment the heading, the evolutionary method fluctuates sharply and falls into the local optimum in the anomalous region, and the traditional LSTM has a certain escape capability due to the combination of the historical data, but due to the lack of the attention mechanism, resulting in a consistent level of attention to the input sequence, and cannot accomplish the navigation task in a limited iteration process. We further analyze the performance of three methods through the convergence of geomagnetic elements.

As is shown in Fig. 11(a) depicts the convergence geomagnetic elements of Attention-DR in Trajectory 1, Fig. 11(b) shows the convergence geomagnetic elements of evolutionary method in Trajectory 2, and Fig. 11(c) shows the convergence geomagnetic elements of original LSTM method in Trajectory 3. Prior to reaching the magnetic anomaly region, both Attention-DR, evolutionary method and original LSTM method maintain stable headings, and the geomagnetic elements continue to converge. When approaching the edge of the magnetic anomaly region, the changes in D and I become less significant, making it challenging for both methods to determine whether they have entered the anomaly area. As a result, they continue to navigate as if in the normal region, causing the heading to deviate slightly towards the anomaly area. As more anomaly information is collected, the Attention-DR method starts utilizing historical information to adjust the heading and simultaneously feeds the data from that region into the network for training, predicting the next location of the heading.

By comparing Fig. 11(a), Fig. 11(b) and Fig. 11(c), it can be observed that the key to navigating out of the anomaly region lies in breaking free from the constraints of the geomagnetic gradient sequence limitations and establishing a close relationship between the geomagnetic information, time, and spatial location. This relationship is crucial for inferring heading anomalies with limited information and time. Attention-DR is able to escape the anomaly region and ultimately reach the destination. Although the geomagnetic information exhibits fluctuations during this process, it successfully converges.

C. Simulation with Multi-destination Navigation

In practical underwater navigation applications, there are usually multiple destination access requirements, and the AUV needs to visit multiple destinations in sequence to accomplish the navigation purpose. In this part of the simulation, the navigation is started from destination 1 (22.6°N, 132.95°E) to destination 2 (22.1°N, 135.97°E), destination 3 (20.3°N, 134.57°E), and destination 4 (19.5°N, 133.5°E), respectively. The AUV will visit these positions in order and then return to destination 1. The performances of the Attention-DR are compared with the evolutionary method, and the simulation setup parameters are consistent with Section IV. A. The simulation results are shown in Fig. 12, where Trajectory 1 is the navigation path of the Attention-DR and Trajectory 2 is the navigation path of the evolutionary method. The termination condition for determining the destination of the AUV arrival is related to the geomagnetic information of the actual destination. When the AUV approaches the vicinity of the destination, the Attention-

DR method can be combined with other navigation methods such as visual navigation and terrain navigation to further enhance the navigation accuracy.

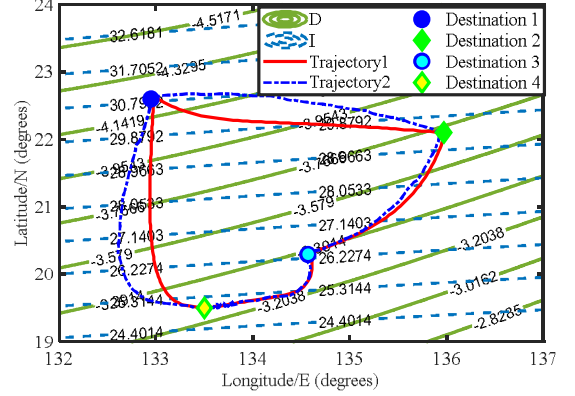


Fig. 12 Simulation with multi-destination navigation.

From Fig. 12, it is evident that both the Attention-DR and evolutionary method are capable of achieving multi-destination navigation. To more accurately estimation the performance of these methods, several common estimation metrics were utilized, and the result are shown in Fig. 13. These metrics were used in conjunction with the visual results depicted in Fig. 12 to demonstrate the effectiveness of the Attention-DR methods. The estimation metrics of iterations can reflect the speed at which the methods approach the destination. The total distance traveled Kilometers (radians) and the ideal distance Kilometers (radians), can reflect how far the AUV has sailed during the navigation process, and the closer to the ideal distance indicates that the method is more efficient. In addition, the variance of the heading angle is utilized to reflect the fluctuation of the heading, thus comparing the stability of the navigation process.

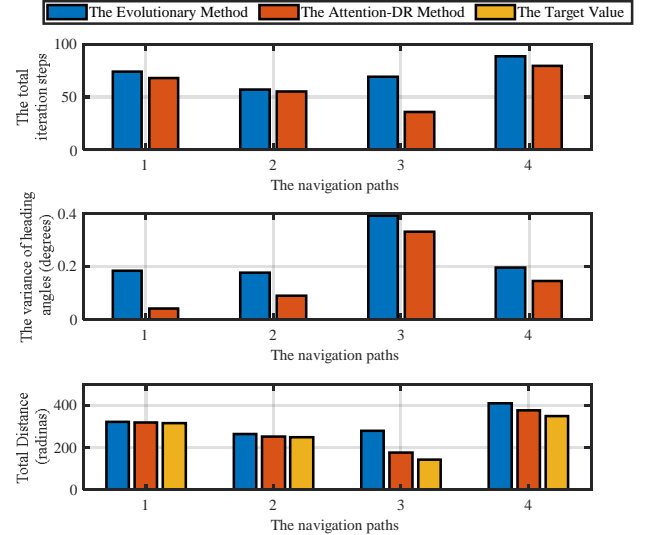


Fig. 13 Statistical chart of simulation results.

From Fig. 13, it can be observed that the Attention-DR method uses fewer iterations to reach the target in all four navigation stages. This reduction is particularly significant in the third stage. Fig. 12 demonstrates that the evolutionary method may exhibit ineffective searches near the destination. Through quantitative analysis, the Attention-DR method

achieves a 20.13% reduction in the number of iterations throughout the entire navigation task. Furthermore, from the variance of the heading angle, it is evident that the Attention-DR method exhibits smaller dispersion, indicating a more stable heading during the navigation process. This advantage is reflected in the entire traveled distance. A more stable heading leads to a shorter total distance traveled and brings the AUV closer to the ideal distance. Through quantitative analysis, the Attention-DR method achieves a 11.71% reduction in traveled distance, being only 6.5% longer than the ideal distance in long-distance geomagnetic navigation.

In conclusion, the Attention-DR method, inspired by biological migration and driven by the proposed TA-LSTM neural network, demonstrates effectiveness and stability in navigation when lacking prior geomagnetic information. By utilizing the temporal attention mechanism to the historical data in both time and location, the Attention-DR method overcomes the limitations of traditional geomagnetic navigation methods that rely on prior maps. Furthermore, it exhibits the capability to navigate in geomagnetic field anomaly regions, the Attention-DR method updates the heading angle, eliminating the need for prior geomagnetic maps. The effectiveness and stability of the Attention-DR method have been verified through simulation experiments.

V. CONCLUSION

This article proposed a bionic geomagnetic navigation for autonomous underwater vehicle with temporal attention-based data-driven dead reckoning. By using the TA-LSTM neural network, Attention-DR utilizes a temporal attention mechanism to compute the heading angle driven by the historical geomagnetic data obtained along the navigation path and the geographical location, to achieving efficient and stable navigation in the absence of priori geomagnetic information. The feasibility and stability of the Attention-DR method are validated by conducting real-time retrieval using the WMM2020 geomagnetic model and an anomaly region composed of multi-modal functions. This study addresses the issues of low search efficiency, high heading fluctuations, and susceptibility to magnetic anomalies in evolutionary methods. To tackle these challenges, a TA-LSTM network is proposed that successfully combines limited historical data in both time and geographical location. It predicts the variation trend of the magnetic field along the navigation route and integrates it with actual magnetic field data to correct the heading angle, thereby improving navigation efficiency and enhancing resistance to interference. The simulation findings provide that the proposed method effectively navigates the AUV towards its intended destination and exhibits good performance in the presence of unknown magnetic field interference.

REFERENCES

- [1] C. Shen *et al.*, "Seamless GPS/Inertial Navigation System Based on Self-Learning Square-Root Cubature Kalman Filter," *IEEE Transactions on Industrial Electronics*, vol. 68, no. 1, pp. 499-508, Jan. 2021, doi: 10.1109/TIE.2020.2967671.
- [2] J. W. Choi, A. V. Borkar, A. C. Singer and G. Chowdhary, "Broadband Acoustic Communication Aided Underwater Inertial Navigation System," *IEEE Robotics and Automation Letters*, vol. 7, no. 2, pp. 5198-5205, April 2022, doi: 10.1109/LRA.2022.3154004.
- [3] J. Melo and A. Matos, "Survey on advances on terrain based navigation for autonomous underwater vehicles," *Ocean Engineering*, vol. 139, pp. 250-264, 2017, doi: 10.1016/j.oceaneng.2017.04.047.
- [4] Z. Wang, Y. Huang, M. Wang, J. Wu and Y. Zhang, "A Computationally Efficient Outlier-Robust Cubature Kalman Filter for Underwater Gravity Matching Navigation," *IEEE Transactions on Instrumentation and Measurement*, vol. 71, pp. 1-18, 2022, no. 8500418, doi: 10.1109/TIM.2022.3141153.
- [5] J. Golden, "Terrain Contour Matching (TERCOM): A Cruise Missile Guidance Aid," *Image Processing for Missile Guidance*, SPIE, vol. 238, pp. 10-18, 1980, doi: 10.1117/12.959127.
- [6] P. Ding and X. Cheng, "A new Contour-Based combined matching algorithm for underwater Terrain-Aided strapdown inertial navigation system," *Measurement*, vol. 202, no. 111870, 2022, doi: 10.1016/j.measurement.2022.111870.
- [7] L. You, Z. Yuan, Z. Peng *et al.*, "An improved inertial/wifi/magnetic fusion structure for indoor navigation," *Information Fusion*, vol. 34, pp. 101-119, Mar. 2017, doi: 10.1016/j.inffus.2016.06.004.
- [8] Z. Chen *et al.*, "A New Geomagnetic Matching Navigation Method Based on Multidimensional Vector Elements of Earth's Magnetic Field," *IEEE Geoscience and Remote Sensing Letters*, vol. 15, no. 8, pp. 1289-1293, Aug. 2018, doi: 10.1109/LGRS.2018.2836465.
- [9] N. Xu *et al.*, "An innovative PSO-ICCP matching algorithm for geomagnetic navigation," *Measurement*, vol. 193, no. 110958, Apr. 2022, doi: 10.1016/j.measurement.2022.110958.
- [10] J. Xiao, X. Duan and X. Qi *et al.*, "An improved ICCP matching algorithm for use in an interference environment during geomagnetic navigation," *The Journal of Navigation*, vol. 73, no. 1, pp. 56-74, July 2019, doi: 10.1017/S0373463319000535.
- [11] Q. Wang, C. Zheng and P. Wu *et al.*, "Geomagnetic/inertial navigation integrated matching navigation method," *Heliyon*, vol. 8, no. 11, Nov. 2022, doi: 10.1016/j.heliyon.2022.e11249.
- [12] N. Putman and K. Lohmann, "Compatibility of magnetic imprinting and secular variation," *Current Biology*, vol. 18, no. 14, pp. 596-597, July 2008, doi: 10.1016/j.cub.2008.05.008.
- [13] K. Lohmann, N. Putman and C. Lohmann, "Geomagnetic imprinting: A unifying hypothesis of long-distance natal homing in salmon and sea turtles," *Proceedings of the National Academy of Sciences*, vol. 105, no. 49, pp. 19096-19101, July 2008, doi: 10.1073/pnas.0801859105.
- [14] N. Putman, "Animal Navigation: Seabirds Home to a Moving Magnetic Target," *Current Biology*, vol. 30, no. 14, pp. 802-804, July 2020, doi: 10.1016/j.cub.2020.05.061.
- [15] J. Gould, "Animal Navigation: A Map for All Seasons," *Current Biology*, vol. 24, no. 4, pp. 153-155, Feb. 2014, doi: 10.1016/j.cub.2014.01.030.
- [16] L. Boles and K. Lohmann, "True navigation and magnetic maps in spiny lobsters," *Nature*, vol. 421, no. 6918, pp. 60-63, Jan. 2003, doi: 10.1038/nature01226.
- [17] L. Jones, N. Putman and J. Stephenson *et al.*, "A Magnetic Map Leads Juvenile European Eels to the Gulf Stream," *Current Biology*, vol. 27, no. 8, pp. 1236-1240, Apr. 2017, doi: 10.1016/j.cub.2017.03.015.
- [18] J. Fischer, M. Freake and S. Borland *et al.*, "Evidence for the use of magnetic map information by an amphibian," *Animal Behaviour*, vol. 62, no. 1, pp. 1-10, July 2001, doi: 10.1006/anbe.2000.1722.
- [19] K. Lohmann, C. Lohmann and L. Ehrhart *et al.*, "Geomagnetic map used in sea-turtle navigation," *Nature*, vol. 428, pp. 909-910, Apr. 2004, doi: 10.1038/428909a.
- [20] A. Pakhomov, A. Anashina and D. Heyers *et al.*, "Magnetic map navigation in a migratory songbird requires trigeminal input," *Scientific Reports*, vol. 8, no. 11975, pp. 1-6, Aug. 2018, doi: 10.1038/s41598-018-30477-8.
- [21] X. Qi *et al.*, "Bioinspired In-Grid Navigation and Positioning Based on an Artificially Established Magnetic Gradient," *IEEE Transactions on Vehicular Technology*, vol. 67, no. 11, pp. 10583-10589, Nov. 2018, doi: 10.1109/TVT.2018.2866428.
- [22] B. Taylor, K. Lohmann and L. Havens *et al.*, "Long-distance transequatorial navigation using sequential measurements of magnetic inclination angle," *Journal of the Royal Society Interface*, vol. 18, no. 174, Jan. 2021, doi: 10.1098/rsif.2020.0887.
- [23] Y. H. Kim, H. J. Kim and J. H. Lee *et al.*, "Sequential batch fusion magnetic anomaly navigation for a low-cost indoor mobile robot," *Measurement*, vol. 213, no. 112706, May 2023, doi: 10.1016/j.measurement.2023.112706.

IEEE TRANSACTIONS ON CYBERNETICS

- [24]A. J. Canciani, "Magnetic navigation on an F-16 aircraft using online calibration," *IEEE Transactions on Aerospace and Electronic Systems*, vol. 58, no.1, pp. 420-434, Feb. 2022, doi: 10.1109/TAES.2021.3101567.
- [25]J. Zhang, T. Zhang and H. S. Shin *et al.*, "Geomagnetic Gradient-Assisted Evolutionary Algorithm for Long-Range Underwater Navigation," *IEEE Transactions on Instrumentation and Measurement*, vol. 70, no. 2503212, pp. 1-12, Oct. 2021, doi: 10.1109/TIM.2020.3034966.
- [26]Y. Zhang, X. Liu, M. Luo and C. Yang, "Bio-Inspired Approach for Long-Range Underwater Navigation Using Model Predictive Control," *IEEE Transactions on Cybernetics*, vol. 51, no. 8, pp. 4286-4297, Aug. 2021, doi: 10.1109/TCYB.2019.2933397.
- [27]S. Wang, Z. Qiu, P. Huang, X. Yu *et al.*, "A Bioinspired Navigation System for Multirotor UAV by Integrating Polarization Compass/Magnetometer/INS/GNSS," *IEEE Transactions on Industrial Electronics*, vol. 70, no. 8, pp. 8526-8536, Aug. 2023, doi: 10.1109/TIE.2022.3212421.
- [28]S. Maus and H. Luhr, "Signature of the quiet-time magnetospheric magnetic field and its electromagnetic induction in the rotating Earth," *Geophysical Journal International*, vol. 168, no. 3, pp. 755-763, Sep. 2005, doi: 10.1111/j.1365-246X.2005.02691.x.
- [29]G. Glatzmaier and P. Roberts, "Rotation and Magnetism of Earth's Inner Core," *Science*, vol. 274, no. 5294, pp. 1887-1891, Dec. 1996, doi: 10.1126/science.274.5294.1887.
- [30]A. Chulliat, W. Brown and P. Alken *et al.*, "The US/UK world magnetic model for 2020-2025: Technical report," National Centers for Environmental Information, National Centers for Environmental Information, USA, 2020, doi: 10.25923/ytk1-yx35.
- [31]P. Alken, E. Thebaud and C. D. Beggan *et al.*, "International Geomagnetic Reference Field: the thirteenth generation," *Earth Planets Space*, vol. 73, no. 49, May. 2020, doi: 10.1186/s40623-020-01288-x.
- [32]K. G. Ivanov and P. Petrushev, "Fast and accurate evaluation of geomagnetic field elements at arbitrary points in space," *Geophysical Journal International*, vol. 224, no. 1, pp. 181-190, Jan. 2021, doi: 10.1093/gji/ggaa439.
- [33]Y. Wu, Y. Li, W. Li, H. Li and R. Lu, "Robust Lidar-Based Localization Scheme for Unmanned Ground Vehicle via Multisensor Fusion," *IEEE Transactions on Neural Networks and Learning Systems*, vol. 32, no. 12, pp. 5633-5643, Dec. 2021, doi: 10.1109/TNNLS.2020.3027983.
- [34]A. Komolkin, P. Kupriyanov and A. Chudin *et al.*, "Theoretically possible spatial accuracy of geomagnetic maps used by migrating animals," *Journal of the Royal Society Interface*, vol. 14, no. 128, Mar. 2017, doi: 10.1098/rsif.2016.1002.
- [35]L. Luhr, C. Xiong and N. Olsen *et al.*, "Near-Earth Magnetic Field Effects of Large-Scale Magnetospheric Currents," *Space Science Reviews*, vol. 206, pp. 521-545, Mar. 2017, doi: 10.1007/s11214-016-0267-y.
- [36]Q. Fu, S. Li and Y. Liu *et al.*, "Information-reusing alignment technology for rotating inertial navigation system," *Aerospace Science and Technology*, vol. 99, no. 105747, Apr. 2020, doi: 10.1016/j.ast.2020.105747.
- [37]B. Liu, S. Wei, J. Lu and J. Wang *et al.*, "Fast Self-Alignment Technology for Hybrid Inertial Navigation Systems Based on a New Two-Position Analytic Method," *IEEE Transactions on Industrial Electronics*, vol. 67, no. 4, pp. 3226-3235, Apr. 2020, doi: 10.1109/TIE.2019.2910045.
- [38]J. Xu, H. He, F. Qin and L. Chang, "A Novel Autonomous Initial Alignment Method for Strapdown Inertial Navigation System," *IEEE Transactions on Instrumentation and Measurement*, vol. 66, no. 9, pp. 2274-2282, Sept. 2017, doi: 10.1109/TIM.2017.2692311.
- [39]S. Hochreiter and J. Schmidhuber, "Long Short-Term Memory," *Neural Computation*, vol. 9, no. 8, pp. 1735-1780, Nov. 1997, doi: 10.1162/neco.1997.9.8.1735.
- [40]K. Zhu, Y. Li and W. Mao *et al.*, "LSTM enhanced by dual-attention-based encoder-decoder for daily peak load forecasting," *Electric Power Systems Research*, vol. 208, no. 107860, Jul. 2022, doi: 10.1016/j.epsr.2022.107860.
- [41]J. E. Boström, S. Åkesson and T. Alerstam, "Where on earth can animals use a geomagnetic bi-coordinate map for navigation," *Ecography*, vol. 35, no. 11, pp. 1039-1047, Aug. 2012, doi: 10.1111/j.1600-0587.2012.07507.x.
- [42]E. A. Michael, "Vector Solutions for Great Circle Navigation," *The Journal of Navigation*, vol. 58, no.3, pp. 451-457, Sep. 2005, doi: 10.1017/S0373463305003358.
- [43]J. Qin, Y. Zhang and S. Fan *et al.*, "Multi-task short-term reactive and active load forecasting method based on attention-LSTM model,"

International Journal of Electrical Power & Energy Systems, 2022, 135: 107517.



Songnan Yang (Student Member, IEEE) received the M.S. degree in Control Science and Engineering in 2020 from Xi'an University of Technology, Xi'an, China. He is currently pursuing the Ph.D. degree with Xi'an University of Technology in Xi'an, China.

His current research interests include geomagnetic navigation.



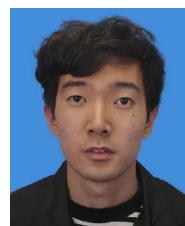
Xiaohui Zhang received the B.S. degree in Industrial Automation in 1995, the M.S. degree in Control Science and Engineering in 2002, and the Ph.D. degree in 2009, all from Xi'an University of Technology, Xi'an, China.

He is currently a Professor of Information and Control Department at Xi'an University of Technology, Xi'an, China. His recent research interests include advanced navigation, signal processing and pattern recognition.



Ding Liu (Member, IEEE) received the B.S. and M.S. degrees from the Xi'an University of Technology, Xi'an, China, in 1982 and 1987, respectively, and the Ph.D. degree from Xi'an Jiaotong University, Xi'an, in 1997.

He is currently a Professor of the Xi'an University of Technology. He has published more than 100 papers in IEEE Transactions on Signal Processing, IEEE Transactions on Control of Network Systems, IEEE Transactions on Antennas and Propagation, and IEEE Sensors Journal et.al. His research interests include large-scale decentralized optimization, complex system's modeling and control, intelligent robot control, digital signal processing, and intelligent control theory.



Wenqi Bai received the M.S. degree in Control Science and Engineering in 2021 from Xi'an University of Technology, Xi'an, China. He is currently pursuing the Ph.D. degree in with Xi'an University of Technology in Xi'an, China.

His current research interests include geomagnetic navigation and reinforcement learning.



Fan Liu received the M.S. degree in Control Science and Engineering in 2022 from Qufu Normal University, Qufu, China. She is currently pursuing the Ph.D degree with Xi'an University of Technology in Xi'an, China.

Her current research interests include the complex system modeling and adaptive control.